

N.m.r., d.s.c., t.m.a. and high-pressure electrical-conductivity studies in solid, crosslinked dimethylsiloxane–ethylene-oxide copolymer networks containing sodium

M. C. Wintersgill, J. J. Fontanella and M. K. Smith

Physics Department, US Naval Academy, Annapolis, MD 21402, USA

and S. G. Greenbaum and K. J. Adamić

Physics Department, Hunter College of CUNY, New York, NY 10021, USA

and C. G. Andeen

Physics Department, Case Western Reserve University, Cleveland, OH 44106, USA

(Received 14 August 1986; accepted 17 November 1986)

Audio frequency electrical conductivity and ^{23}Na n.m.r. studies have been made on solid, crosslinked dimethylsiloxane–ethylene-oxide copolymer networks containing sodium. Electrical measurements were made in vacuum over the temperature range 5 K to 380 K and at pressures up to 0.65 GPa over the temperature range 230 K to 380 K. The electrical conductivity for the complexed material and the electrical relaxation time associated with the α -relaxation in the uncomplexed material exhibit Vogel–Tamman–Fulcher (V.T.F.) or Williams–Landel–Ferry (W.L.F.) behaviour. From a V.T.F. analysis of the electrical conductivity, the activation energy, E_a , is found to be about 0.11 eV and T_0 is found to be about 45°C below the ‘central’ glass transition temperature as determined by both d.s.c. and t.m.a. Also, T_0 is found to increase by about 50 K GPa^{-1} and E_a to increase significantly with pressure. In addition, the high-pressure studies show that the activation volume associated with electrical conductivity decreases from 44 to 23 $\text{cm}^3 \text{mol}^{-1}$ over the temperature range 262 K to 323 K. The ^{23}Na n.m.r. measurements reveal the presence of both bound and mobile sodium species, the relative concentrations of which change by about a factor of 10 over the temperature range -100°C to $+100^\circ\text{C}$. Broadening of the bound ^{23}Na line above room temperature suggests the possible presence of ion pairs or higher aggregates in the complex.

(Keywords: n.m.r.; d.s.c.; t.m.a.; sodium containing copolymer; dimethylsiloxane–ethane-oxide copolymer; network)

INTRODUCTION

Poly(dimethylsiloxane–ethylene-oxide) poly(DMS–EO) copolymers complexed with alkali metal salts have been receiving attention as solid electrolytes^{1–5}. The primary reason for this, of course, is that in general siloxanes have very low glass transition temperatures and this feature is known to enhance ionic conductivity. In a recent paper⁵, several of the present authors have reported the synthesis of a highly crosslinked poly(DMS–EO) network containing sodium. In addition, various studies, including differential scanning calorimetry (d.s.c.), ^{23}Na nuclear magnetic resonance (n.m.r.) and vacuum electrical conductivity were presented. It was shown that the room-temperature electrical conductivity was relatively large and that the complex had the advantages of being highly amorphous and stable. Consequently, the material is of interest as a potential solid electrolyte.

In the present paper, results for a differently prepared material are reported. In addition, new types of measurements have been made, including thermo-mechanical analysis (t.m.a.) and high-pressure electrical conductivity.

EXPERIMENTAL

Preparation of a crosslinked poly(DMS–EO): NaCF_3COO complex has been described in detail elsewhere⁵. In the present study the composition was slightly altered by adding approximately 33% (by mass) PDMS to the poly(DMS–EO) copolymer while keeping the EO/Na ratio fixed at approximately 8:1. This did not appear to improve the conductivity significantly, although the modified material did exhibit better mechanical flexibility. In addition, differences were noted in some of the thermal properties and n.m.r. linewidths, as discussed later.

^{23}Na n.m.r. measurements were made at 81 MHz by making use of standard pulse techniques. Fourier transform spectra were recorded after accumulation of 1000 free induction decays (FIDs). Linewidths and relative intensities of the two resolvable lineshape components were extracted from the FIDs by selective saturation and subtraction, as discussed below.

Audio frequency complex-impedance–electrical relaxation measurements have been made with a fully automated spectrometer. The key element in the

measurements is a CGA-82 microprocessor-controlled bridge operating at seventeen frequencies from 10 to 10^5 Hz. Vacuum measurements were made in a Precision Cryogenics CT-14 dewar controlled by a Lake Shore Cryotronics DRC-82 temperature controller with a silicon diode sensor. The high-pressure measurements were made in a pressure vessel by using Fluorinert (3M Co.) FC-77 electronic liquid as the high-pressure fluid. For the electrical measurements, gold electrodes were vacuum-evaporated onto the surfaces of the material in either a three-terminal or two-terminal configuration. The samples were about 1 mm thick and the electrodes about 4 mm in diameter. D.s.c. and t.m.a. measurements were made with a computer-controlled DuPont 990 console coupled with a 910 DSC and 943 TMA.

RESULTS

Thermal analysis

Typical penetration t.m.a. results for poly(DMS-EO) complexed with sodium trifluoroacetate are shown in Figure 1. The primary feature of interest in the present work is the transition occurring at about -55°C . Since the material begins to soften at that temperature, the event is attributed to the glass transition. Further evidence is shown in Figure 2, where the d.s.c. data are plotted. A feature typical of a glass transition is observed to begin at about -67°C and end at about -47°C . The 'central' glass transition temperature, -57°C , is about 5°C lower than for the higher EO-content siloxane polymer studied previously⁵. The centre of the d.s.c. glass transition occurs at approximately the same temperature as the low-temperature t.m.a. softening.

A second feature is observed in the d.s.c., which was not observed previously⁵. Specifically, there is an event at about 0°C . A corresponding feature was not observed in t.m.a. studies. Heating the sample at about 130°C decreased the temperature of this feature to about -15°C . Because of the variability of the temperature of this feature, it is not attributable to water. It is, in fact, similar to the d.s.c. scans of Fish *et al.*³ for an uncrosslinked ion containing siloxane polymer, and thus may somehow be associated with the absence of crosslinking in regions of the material.

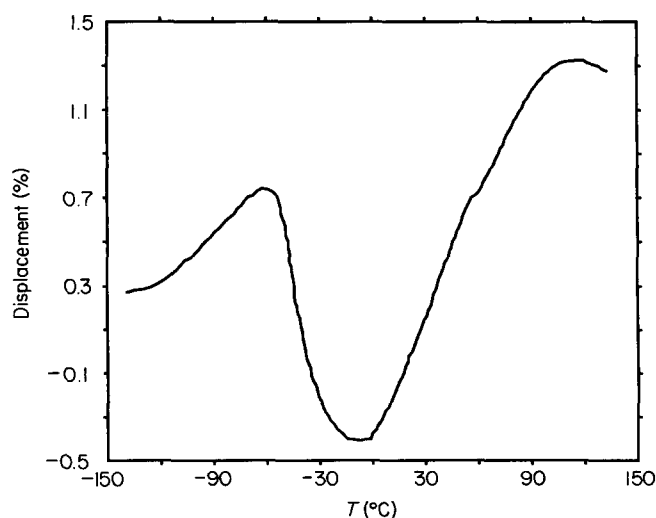


Figure 1 T.m.a. plot showing the glass transition at about -55°C . The data were taken at 5 K min^{-1} .

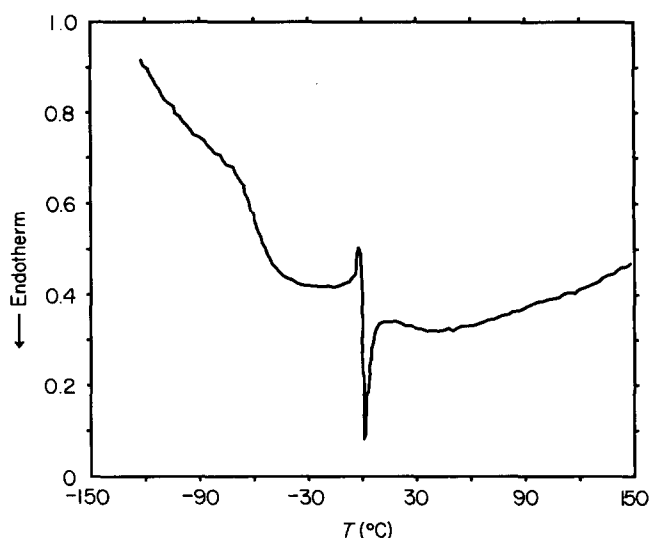


Figure 2 D.s.c. plot showing the glass transition at about -55°C . The data were taken at 10 K min^{-1} .

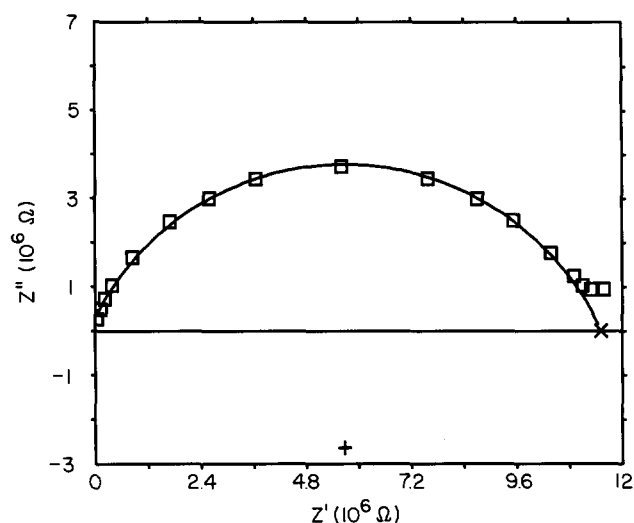


Figure 3 Complex-impedance plot at 254 K. The 'plus sign' shows the centre of the depressed Cole-Cole arc and the 'multiplication sign' represents the bulk resistance of the sample. The squares represent the datum points and the solid line is the best-fit Cole-Cole equation (equation (1)).

Electrical conductivity

A typical low-temperature complex-impedance plot is shown in Figure 3. The data were analysed by using a Cole-Cole distribution⁶

$$Z^* = \frac{Z_0}{1 + (i\omega\tau_0)^{1-\alpha}} \quad (1)$$

where Z_0 , τ_0 , and α are the fitting parameters. As temperature increases, less of a semicircle is observed together with a slanted vertical line at lower frequencies representing blocking electrode effects. In most cases, a best-fit of equation (1) to the data was obtained, which allowed values for the bulk resistance of the materials to be determined. For the remaining plots, a combination of the depressed arc and slanted vertical line was used to determine the bulk resistance.

The conductance values, G , were then used, in conjunction with room-temperature geometrical measurements, to calculate the electrical conductivity from

$$\sigma = Gt/S \quad (2)$$

where t is the thickness and S the surface area. Thermal expansion effects are not included in the data analysis. The results of a typical vacuum data run are shown in Figure 4. The curvature often observed for amorphous polymer systems is apparent. Consequently, the conductivity data were first analysed via the V.T.F. equation⁷

$$\sigma = AT^{-1/2} \exp\{-[E_a/k(T-T_0)]\} \quad (3)$$

with the adjustable parameters A , E_a and T_0 . A non-linear least-squares fit of equation (3) to the data was made and Table 1 contains the best-fit parameters.

It is noted that the vacuum values for T_0 are about 45°C lower than the 'central' T_g s, which were determined by d.s.c. or the softening temperature, as determined by t.m.a. This result is consistent with all previous work by the authors^{5,8,9}. Such results are not unexpected since $T_g - T_0$ is often of the order of 50°C for polymer systems^{10,11}. Further, this phenomenon is consistent with the configurational entropy model^{12,13}, where T_0 is interpreted as the temperature of zero configurational entropy, which would be expected to occur at a much

lower temperature than d.s.c. T_g s. However, this result disagrees with those of other workers¹² for similar materials. Possible reasons for the discrepancy along with details of the data analysis technique used in the present work are given elsewhere⁵.

Next, isothermal data were taken and typical results are shown in Figure 5. The equation

$$\log_{10} \sigma = \log_{10} \sigma_0 + aP + bP^2 \quad (4)$$

was best-fit to the isothermal data and the best-fit parameters are listed in Table 2. The values listed in Table 2 for $\log_{10} \sigma_0$ are those calculated from the vacuum data (i.e. absolute conductivities were not determined for the pressure runs, rather, relative changes were determined and the absolute value normalized to the more accurate vacuum data).

The isothermal studies can also be used to determine activation volumes directly via

$$\Delta V^* = -kTd \ln \sigma / dP \quad (5)$$

The zero-pressure values, those calculated from the slope of the conductivity *versus* pressure plot at $P=0$, are listed

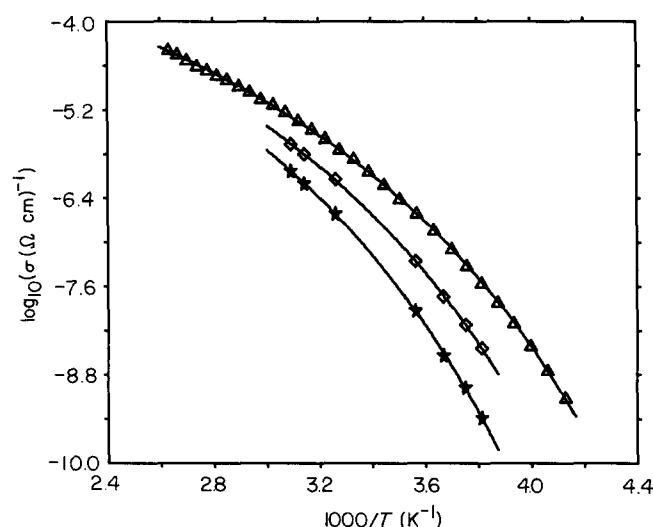


Figure 4 Arrhenius plot of the electrical conductivity data. From top to bottom the data are vacuum (triangles), 0.1 GPa (diamonds), and 0.2 GPa (stars). The solid lines are the best fit V.T.F. equation (3))

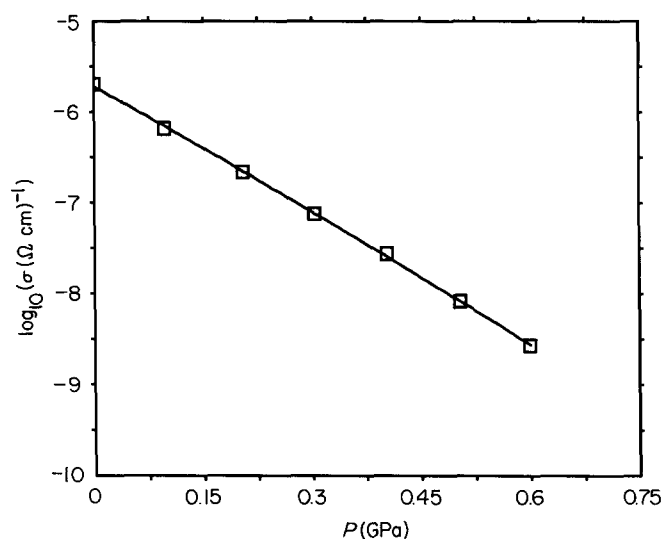


Figure 5 Typical data and best-fit quadratic (equation (4)) for the pressure dependence of electrical conductivity. The data are at 306.6 K

Table 1 Best-fit V.T.F. parameters

	R.m.s. deviation	$\log_{10} A$ ($\Omega \text{ cm}$) ⁻¹ K ^{1/2}	E_a (eV)	T_0 (K)	R.m.s. deviation	$\log_{10} A'$ ($\Omega \text{ cm}$) ⁻¹	E'_a (eV)	T'_0 (K)
Vacuum	0.0120	-0.63	0.102	171.7	0.0130	-2.03	0.097	173.5
0.1 GPa	0.0051	-0.43	0.115	176.7	0.0052	-1.81	0.111	178.1
0.2 GPa	0.0102	-0.26	0.127	181.3	0.0104	-1.63	0.123	182.4

Table 2 Best-fit parameters in equation (4) and activation volumes for isothermal data

Maximum pressure (GPa)	T (K)	R.m.s. deviation	$\log_{10} \sigma_0$ ($\Omega \text{ cm}$) ⁻¹	a (GPa) ⁻¹	b (GPa) ⁻²	ΔV^* (cm ³ mol ⁻¹)
0.15	262.2	0.0031	-7.530	-8.77	-2.21	44.0
0.27	266.5	0.0034	-7.276	-8.19	-1.44	41.8
0.23	272.3	0.0045	-6.968	-7.51	-1.48	39.1
0.30	280.5	0.0078	-6.588	-6.54	-0.70	35.1
0.60	306.6	0.0190	-5.692	-4.44	-0.49	26.1
0.55	317.9	0.0098	-5.405	-3.91	-0.23	23.8
0.40	323.4	0.0073	-5.281	-3.75	+0.17	23.2

in Table 2. The magnitude of the activation volumes is consistent with results for other ion-conducting polymers, and it is clear that they decrease as temperature increases. Also, the curvature of the $\log \sigma$ versus pressure plot, which is related to the parameter b listed in Table 2, is negative at the lowest temperatures, becoming less so as temperature increases. Both results are similar to results for PPO complexed with lithium salts reported previously when the same analysis techniques were used^{8,9}, but opposite to the case of a single-frequency analysis of results on ion-containing PEO presented earlier¹⁴.

Next, the isothermal pressure data were used to generate 0.1 and 0.2 GPa conductivities. The results were best-fit to equation (3) and the parameters are listed in Table 1. Both data and best-fit curves are plotted in Figure 4. It is found that T_0 increases by about 5 K kbar⁻¹. This is between the trends observed for PPO₈LiCF₃SO₃, which showed a shift of about 10 K kbar⁻¹, and PPO₈LiClO₄ and PPO₈LiI, for which the shift was very small. Since glass transitions usually shift several K kbar⁻¹, this result is consistent with the usual assertion that T_0 is somehow associated with T_g . Obviously, the configurational entropy model provides such an interpretation.

Further, it is found that E_a also increases with pressure. As pointed out previously⁹, this provides evidence against 'liquid-like' conductivity in these materials.

Next, the data were analysed in terms of the W.L.F. equation¹¹

$$\log_{10} \frac{\sigma(T)}{\sigma(T_g)} = \frac{C_1(T - T_g)}{C_2 + (T - T_g)} \quad (5)$$

The resultant parameters are listed in Table 3. The values of C_1 and/or C_2 are rather lower than the 'universal' values of 17.4 and 51.6.

Finally, for completeness, the data were analysed via the mathematically equivalent V.T.F. equation in the form

$$\sigma = A' \exp\{-[E_a'/(T - T_0)]\} \quad (6)$$

The results are listed in Table 1. It is interesting that on the basis of the r.m.s. deviation it is equation (3) that best fits the data.

Nuclear magnetic resonance

The ²³Na absorption was previously shown to consist of a relatively narrow line with a short (approximately 1 ms) spin-lattice relaxation time (T_1) superimposed on a long T_1 (approximately 1 s) second-order quadrupole-broadened line⁵. The composite n.m.r. lineshape for the original sample⁵, hereafter denoted as sample A, is shown in Figure 6a. The broken portion represents the absorption spectrum corresponding to the narrow line, which is obtained by saturating the long- T_1 component. The spectra were taken at -76°C, well below T_g , with sequence delays of 10 s and 40 ms for the unsaturated and

saturated lines, respectively. Figure 6b displays both unsaturated and partly-saturated spectra (at $T = -100^\circ\text{C}$) for the present lower-EO-content complex, hereafter denoted as sample B. The primary difference between the two samples appears to be the greater degree of broadening in the broad component of A. In fact, the broad line of B (Figure 6b) is not second-order quadrupole broadened, as determined by the values of the $\pi/2$ pulse widths for each lineshape component. The full-width at half maximum (f.w.h.m.) of the narrow line of B remains relatively constant at approximately 5 kHz until about T_g , then narrows to a minimum of 1 kHz at about -5°C . At higher temperature, the line gradually broadens to about 1.7 kHz as a result of extremely rapid spin-lattice relaxation. The f.w.h.m. of the broad line of B remains between 7 and 10 kHz over the temperature range -100 to 100°C . However, a transition from first- to second-order quadrupole broadening occurs at about 25°C . This is in contrast to the results for sample A, in which the broad component exhibits second-order quadrupole effects over the entire temperature range⁵.

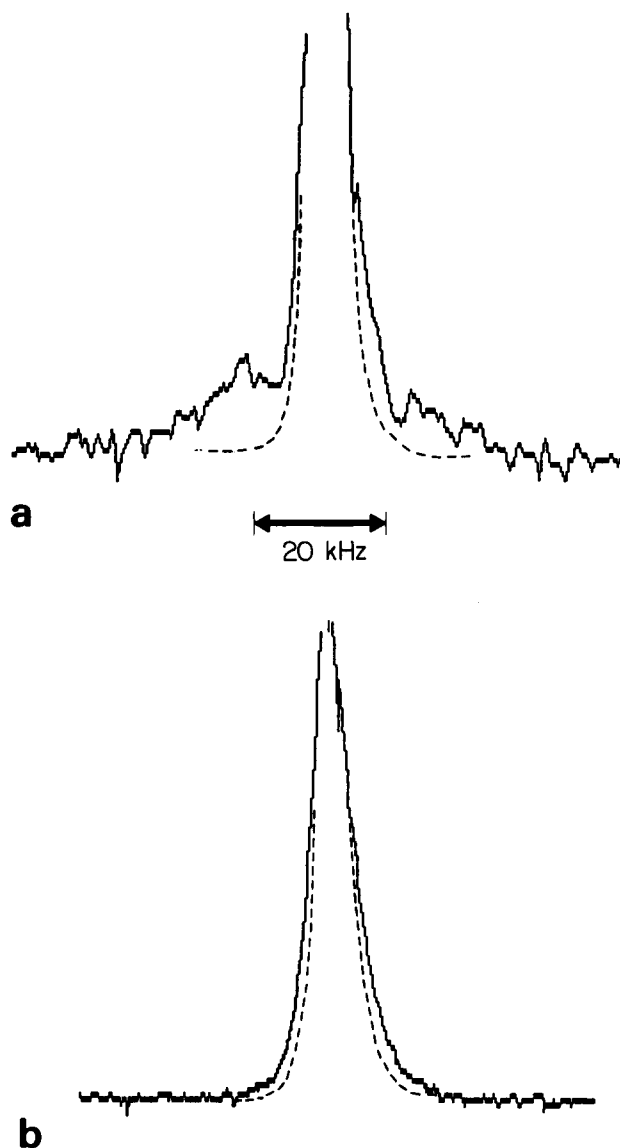


Figure 6 ²³Na n.m.r. absorption spectra for (a) sample A, and (b) sample B (lower EO-content than A). The broken curves in (a) and (b) are spectra obtained with a short sequence delay, in which the broad components are completely saturated

Table 3 D.s.c. results and best-fit W.L.F. parameters

	T_g (K)	C_1	C_2 (K)	$\log_{10} \sigma(T_g)$ ($\Omega \text{ cm}^{-1}$) ⁻¹	R.m.s. deviation
Onset	206	15.0	32.5	-17.0	0.0130
Central	216	11.5	42.5	-13.5	0.0130
End	226	9.3	52.5	-11.3	0.0130

A common feature of samples A and B is the presence of both the broad and narrow lineshape components throughout the temperature range -100°C to 100°C . As the difference between the T_1 values of the two components was always at least a factor of 100^5 , the individual contributions of each line to the composite lineshape, and hence their relative intensities, could be determined easily. The ratio of narrow to broad line intensity as a function of temperature (for sample B) is shown in Figure 7.

The short- T_1 , narrow line has been previously identified with highly mobile Na^+ ions⁵. Among the possible configurations giving rise to the long- T_1 , broad line are sodium ions rigidly bonded to the host polymer chains, and isolated cation-anion pairs or clusters. The presence of ion pairs in conducting polymer complexes has been inferred from a variety of measurements, including vibrational spectroscopy¹⁰ and pulsed field-gradient n.m.r.¹⁵ Conductivity measurements as a function of salt concentration in low molecular weight polyethers suggest that neutral ion pairs and charged ion triplets are the predominant salt species at low salt concentration¹⁶.

The possibility that the ^{23}Na broad line might be associated with ion pairs or higher aggregates is given credence by known quadrupole coupling constants for Na^+ -anion pairs in the gas phase¹⁷. Figure 7 may then be representative of a temperature dependent pair (or aggregate) dissociation process, although the presence of an alternative Na configuration for the broad line, such as bonded to the polymer chains, cannot be ruled out. It is interesting to note that, according to the data in Figure 7, the Na^+ -ion concentration increases by only a factor of 10 from -100°C to $+100^{\circ}\text{C}$, while the conductivity exhibits roughly a five-order of magnitude increase over the same range. So, it appears that large-scale segmental motion of the polymer chains implied by the V.T.F. behaviour of the conductivity plays a much greater role than 'carrier generation' in the transport process. A similar conclusion has been drawn by Watanabe *et al.*¹⁸, who inferred the presence of a weakly temperature-

dependent dissociation process from time-of-flight mobility measurements in Li-PPO complexes.

Although there is considerable uncertainty in the higher-temperature data of Figure 7 (owing to the low signal-to-noise ratio characteristic of the broad line above room temperature), it is clear that the Na^+ -ion concentration (narrow line) does not continue to increase with increasing temperature, at least not at the rate observed at lower temperatures. There is presently no satisfactory explanation for this observation, nor does the high-temperature scatter of the data permit further speculation on this point. The final comment concerns the previously mentioned transition to second-order quadrupole broadening above room temperature. For the n.m.r. frequency employed (81 MHz), second-order broadening implies a quadrupole coupling constant of the order of 1 MHz, which is comparable to that of a Na^+ -anion pair¹⁷. It can be shown¹⁹ that the quadrupole coupling associated with a sodium ion in contact with a neutral ion-pair, i.e. an ion triplet, is somewhat smaller than for a sodium ion in contact with an anion, i.e. an ion pair. So, the presence of a significant number of triplets that are converted to single ions and ion pairs above room temperature could provide an explanation for the observed broadening. Further evidence for or against this simple model will require more accurate narrow/broad ratios as well as better estimates of quadrupole coupling constants from the observed lineshapes.

SUMMARY

In summary, the following results have been obtained.

(a) Vacuum electrical conductivity measurements have been made and analysed in terms of V.T.F. and W.L.F. equations. The most important result is that for the V.T.F. equation T_0 is found to be about 45°C below the 'central' T_g . This is consistent with the usual behaviour of these quantities and is predicted by the configurational entropy model. For the W.L.F. equation, the values of C_1 and/or C_2 are found to be slightly lower than the 'universal' values.

(b) High-pressure electrical conductivity measurements have also been made and a V.T.F. analysis shows that T_0 increases by about 50 K GPa^{-1} and E_a increases significantly. In addition, the activation volume associated with the electrical conductivity decreases as temperature increases, as expected.

(c) ^{23}Na n.m.r.-determined mobile/bound sodium ratios exhibit a factor of 10 increase over the temperature range -100°C to $+100^{\circ}\text{C}$, in contrast with the 10^5 increase in conductivity over the same range. Thus carrier generation plays a relatively minor role in the transport mechanism.

ACKNOWLEDGEMENTS

The authors acknowledge Mr Yiu Sun Pak and Ms Meng Chiao for assistance with n.m.r. measurements and data analysis. This research was supported in part by the Office of Naval Research and the PSC-CUNY Research Award Program.

REFERENCES

- 1 Nagaoka, K., Naruse, H., Shinohara, I. and Watanabe, M. *J. Polym. Sci., Polym. Lett. Edn.* 1984, **22**, 659

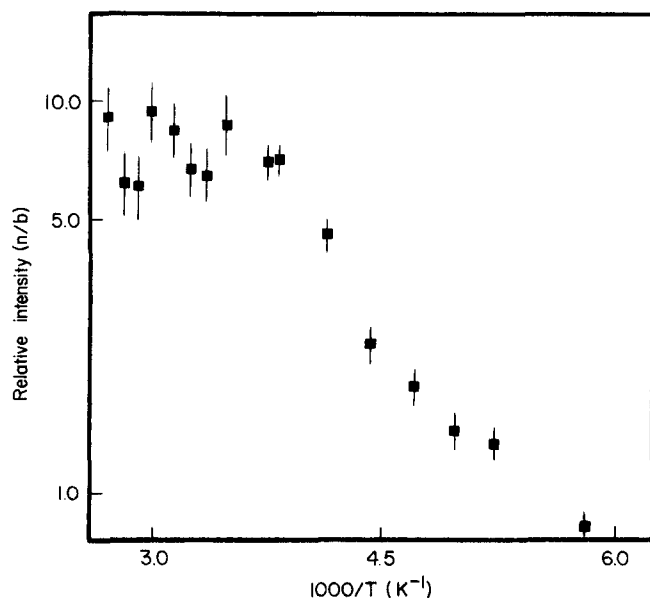


Figure 7 Reciprocal temperature plot of narrow (n)/broad (b) line intensity ratios for sample B

- 2 Bouridah, A., Dalard, F., Deroo, D., Cheradame, H. and Le Nest, J. F. *Solid State Ionics* 1985, **15**, 233
- 3 Fish, D., Khan, I. M. and Smid, J. *Makromol. Chem., Rapid Commun.* 1986, **7**, 115
- 4 Hall, P. G., Davis, G. R., McIntyre, J. E., Ward, I. M., Bannister, D. J. and Le Brocq, K. M. F. *Polymer* 1986, **27** (Commun.), 98
- 5 Adamić, K. J., Greenbaum, S. G., Wintersgill, M. C. and Fontanella, J. J. *J. Appl. Phys.* 1986, **60**, 1342
- 6 Cole, K. S. and Cole, R. H. *J. Chem. Phys.* 1941, **9**, 341
- 7 Vogel, H. *Physik Z.* 1921, **22**, 645; Tammann, V. G. and Hesse, W. *Z. Anorg. Allg. Chem.* 1926, **156**, 245; Fulcher, G. S. *J. Am. Ceram. Soc.* 1925, **8**, 339
- 8 Fontanella, J. J., Wintersgill, M. C., Calame, J. P., Smith, M. K. and Andeen, C. G. *Solid State Ionics* 1986, **18/19**, 253
- 9 Fontanella, J. J., Wintersgill, M. C., Smith, M. K., Semancik, J. and Andeen, C. G. *J. Appl. Phys.* 1986, **60**, 2665
- 10 Papke, B. L., Ratner, M. A. and Shriver, D. F. *J. Electrochem. Soc.* 1982, **129**, 1694
- 11 Angell, C. A. *Solid State Ionics* 1983, **9/10**, 3
- 12 Gibbs, J. H. and DiMarzio, E. A. *J. Chem. Phys.* 1958, **28**, 373
- 13 Adam, G. and Gibbs, J. H. *J. Chem. Phys.* 1965, **43**, 139
- 14 Fontanella, J. J., Wintersgill, M. C., Calame, J. P., Pursel, F. P., Figueroa, D. R. and Andeen, C. G. *Solid State Ionics* 1983, **9/10**, 1139
- 15 Bhattacharja, S., Smoot, S. W. and Whitmore, D. H. *Solid State Ionics* 1986, **18/19**, 306
- 16 Hall, P. G., Davies, G. R., Ward, I. M. and McIntyre, J. E. *Polymer* 1986, **27** (Commun.), 100
- 17 Semin, G. K., Barbushkina, T. A. and Yakobson, G. G. 'Nuclear Quadrupole Resonance in Chemistry', John Wiley and Sons, New York, 1975
- 18 Watanabe, M., Sanui, K., Ogata, N., Kobayashi, T. and Ohtaki, Z. *J. Appl. Phys.* 1985, **57**, 123
- 19 Cohen, M. H. and Reif, F., 'Solid State Physics' (Eds. F. Seitz and D. Turnbull), Academic Press, New York, 1957